

Green Downstream Processing Method for Xylooligosaccharide Purification and Assessment of Its Prebiotic Properties

Rutuja Murlidhar Sonkar, Pravin Savata Gade, Sandeep N. Mudliar, and Praveena Bhatt*

Cite This: *ACS Omega* 2023, 8, 42815–42826

Read Online

ACCESS |



Metrics & More

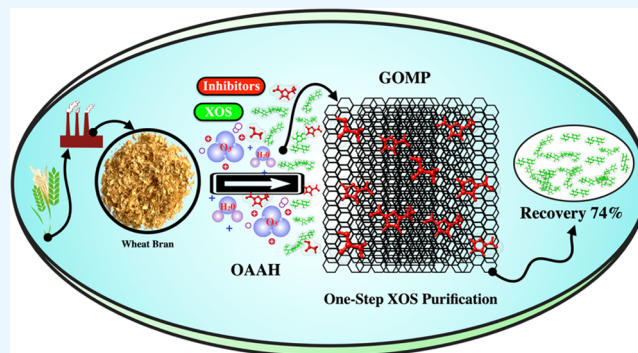


Article Recommendations



Supporting Information

ABSTRACT: Xylooligosaccharides (XOS) obtained from lignocellulosic biomass after autohydrolysis primarily consist of lignin-derived impurities and autogenerated inhibitors like furfural, hydroxymethylfurfural, and acetic acid. In this study, graphene oxide-mediated purification (GOMP), a novel and environmentally friendly downstream processing method, was developed for the purification of XOS from hydrolysate obtained after ozone-assisted autohydrolysis of wheat bran. GOMP resulted in appreciable recovery of total XOS from the hydrolysate ($73.87 \pm 4.25\%$, DP2–6) with near complete removal of autogenerated inhibitors (furfural 85.42%, HMF 87.38%, and acetic acid 84.0%). Recovery of XOS by GOMP was higher than the conventional membrane purification technique ($44.07 \pm 0.92\%$) and activated charcoal treatment ($72.76 \pm 0.84\%$) along with comparatively higher removal of inhibitor compounds. GOMP results in the selective adsorption of inhibitors on the graphene oxide matrix from the XOS-rich hydrolysate, resulting in its purification and concentration. The prebiotic function of the obtained XOS fractions (DP2–4.48%, DP3–39.69%, DP4–36.13%, DP5–8.38%, and DP6–13.10%) was evaluated, indicating the growth stimulation of tested probiotic cultures and differential utilization of XOS oligomers DP3 and DP4 and complete consumption of DP2, DP5, and DP6 along with short-chain fatty acids as a major fermentation product. These findings suggest that GOMP, which employs a common substance (i.e., graphene oxide) used in water treatment, exhibits potential as an efficient and economically viable single-step methodology for XOS purification.



1. INTRODUCTION

The lignocellulosic agro-industry waste is the most abundant and renewable source of sustainable energy for mankind. Lignocellulosic materials which are mainly composed of lignin, cellulose, and hemicellulose are promising economical resources for obtaining bioenergy, food additives, and fermentable sugars.¹ The bioactive-rich agro-industry waste utilization for the production of value-added products not only reduces the production cost but also minimizes the pollution load from the environment.² This lignocellulosic waste can be valorized by the production of the oligosaccharide and ultimately contribute to cyclic bioeconomics.³

Xylooligosaccharide (XOS) is a nondigestible functional product derived through chemical, physical, enzymatic, and thermal degradation of xylan, obtained from hemicellulose-rich biomass.^{4,5} Hemicellulose is a polysaccharide made of xylose, galactose, arabinose, mannose, and glucuronic acid.⁶ The agro-industrial waste sources of hemicellulose that can be used for XOS production are wheat bran, rice bran, bamboo, sorghum husk, coconut husk, wheat straw, sugar cane straw, sugar cane bagasse, etc.⁷ Global wheat production increased by 1.9% from 2021 and is forecasted to reach 777 million tons in 2022 according to the Food and Agricultural Organization, United States (FAO).⁸ Approximately, 0.25 tons of wheat bran are

produced per ton of processed wheat, which is equivalent to 14–16% of cereal kernel.⁹

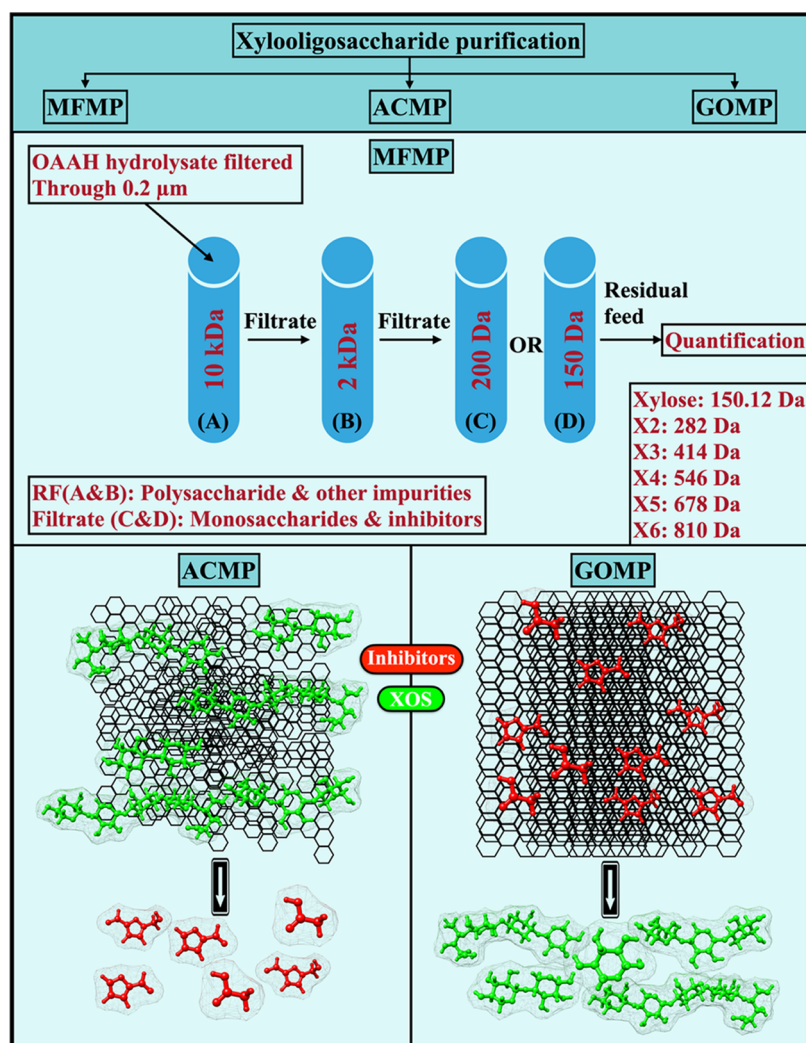
XOS production is mainly preferred by thermal/enzymatic treatment or a combination of these treatments because of their green synthesis.¹⁰ Moreover, the obtained XOS is highly stable against thermal and mechanical stress making it a promising prebiotic candidate to be used in plant-based beverages.¹¹ The chemical methods use extensive alkali/acidic reagents which interfere with downstream processing as well as chemicals used in delignification, leading to the loss of target biomass.^{12,13}

The XOS produced through autohydrolysis mainly contains impurities like monosaccharides, partial degradation of lignin-derived products, derivatives of sugars resulting from dehydration, and condensation of carbohydrates and ash.¹⁴ The mild acidic (H^+) condition in combination with higher

Received: August 4, 2023
Revised: October 5, 2023
Accepted: October 9, 2023
Published: October 31, 2023



Scheme 1. Schematic Representation of Strategies Used for XOS Purification (A) MFMP-Membrane Filtration-Mediated Purification, (B) ACMP-Activated Carbon-Mediated Purification, and (C) GOMP-Graphene Oxide-Mediated Purification



temperature leads to the dehydration of the xylose to furfural.¹⁵ The treatment with activated charcoal (AC) is an efficient process that is conventionally used for the removal of lignin and furfural from the hemicellulose and also delignification of prehydrolysate.¹⁶ In AC, the selective adsorption of lignin impurities from hydrolysate depends mainly on the acidic surface groups and level of microporous nature along with small mesopore diameters of the carbon material while the several basic groups present in carbon restrict the adsorption of XOS.¹⁷ In AC, ethanol is used as an eluant to remove the bound compound of interest, which causes certain downstream processing issues. Residual ethanol in the sample might disrupt downstream applications such as further enzymatic treatments. Ethanol is known to impede enzyme function and influence cell viability in cases in which whole-cell applications are envisaged. The solvent could also interfere with the structural and functional characteristics of the biomolecules.^{18–20} Ethanol removal is quite costly, and utilizing it in large quantities for multiple elutions can greatly increase the overall cost of the process. In membrane filtration, the high input energy, costly membranes, and fouling of inlet membrane, as well as the limited barrier for the movement of ions may require an extension of other separation techniques along with

membrane filtration such as ion exchange and electro-dialysis making the overall operation costly and complicated.^{20,21}

The prebiotic effects of XOS are well-documented in the literature. “Prebiotics are the substrates that are selectively utilized by host microorganisms conferring health benefit”.²² XOS is a prebiotic gaining interest due to its multidimensional effects on human health including its preventive nature in gastrointestinal disorders. XOS selectively stimulates the growth of nonpathogenic microbes, especially the Lactobacillaceae family, and can contribute to making a positive shift in gut microbiota.^{23,24} Almost 70% of the body’s immune response is associated with gut homeostasis, therefore, gut microbiota modulation with prebiotic substrates is gaining interest and XOS stands top in the list.¹¹

In our previous study, we reported a novel ozone-assisted autohydrolysis method for XOS production, which resulted in significantly higher yields of XOS, low inhibitor generation, and prebiotic low DP oligomers.¹⁴ Further to this work, in the present study, we hypothesized that graphene oxide (GO) preferentially interacts with autogenerated inhibitors during OAAH treatment, assisting in the purification and concentration of XOS while also preserving its prebiotic potential by eliminating the inhibitors. To test the hypothesis, we explored the purification of XOS from the obtained hydrolysate using

GO, due to its high recovery. GO is an emergent catalyst and has been used extensively as an adsorbent for the removal of water contaminants (bacteria, heavy metals, mercury, fluoride, copper, and arsenic).²⁵ It has a negatively charged large surface area, thermal stability, mechanical strength, excellent conductivity, and metal-free catalyst.^{26–28}

Moreover, the different groups present on the GO surface are known to impart catalytic activity and lead to the adsorption of different compounds, especially the selective removal of aromatic ring compounds.²⁹ Based on these properties, we hypothesized that GO may be a suitable and efficient adsorbent for the removal of autogenerated inhibitors from autohydrolysis. We compared the developed graphene oxide-based purification (GOMP) method with AC and membrane filtration techniques, which are conventionally used for purification. Furthermore, in order to ensure retention of the prebiotic potential of GOMP-XOS, its growth stimulatory activity on probiotic lactic acid bacteria was investigated. The preferential utilization of the different DP XOS oligomers by the bacteria was also studied, along with the production of bioactive metabolites (SCFAs). The results of this study are presented in the present manuscript.

2. EXPERIMENTAL SECTION

2.1. Chemicals and Reagents. All LAB strains used in this study were *L. rhamnosus*, *L. casei*, *L. acidophilus*, and *L. plantarum* and were cultivated in the de Mann Rogosa Sharpe medium (MRS, Hi-media Lab Pvt. Ltd., India) under microaerophilic conditions for 24 h. For comparative growth analysis, all basal medium components and different carbon sources such as protease peptone, beef extract, polysorbate 80 (Hi-media Lab Pvt. Ltd., India), yeast extract (Sigma Aldrich), sodium acetate (Qualigens), magnesium sulfate, manganese sulfate, triammonium citrate, activated charcoal (Loba Chemie Pvt. Ltd.), dipotassium phosphate (RANKEM), and dextrose (Merck Life Science, India) were procured and used as received.

Reagents used in the analysis of XOS, acetic acid, furfural, hydroxymethylfurfural (HMF), SCFA, and organic acids were of HPLC grade and procured from Sigma Aldrich.

2.2. XOS-Rich Hydrolysate from Ozone-Assisted Autohydrolysis (OAAH). The OAAH treatment was performed according to our previous study.¹⁴ In brief, 3% wheat bran slurry was prepared in a stainless-steel reactor, followed by the treatment with 3% ozone using an air-feed ozone generator (Faraday Ozone, model: A4G). After the treatment, the reactor was closed, and autohydrolysis was performed at a temperature of 110 °C. Further after cooling the reactor, the obtained hydrolysate was centrifuged and the supernatant was stored at –20 °C until further analysis and purification studies.

2.3. XOS Purification. **2.3.1. Membrane Filtration-Mediated Purification (MFMP) of XOS.** The TFC polyamide membranes were cut into 45 mm diameters and soaked in deionized water overnight before the experiment. The filtration cell was filled with the hydrolysate and constantly stirred at 300 rpm with a supply of pressure. The experiments were conducted at room temperature as per Scheme 1. Briefly, the supernatant of hydrolysate was filtered through 0.22 μm syringe filters, and sequential membrane filtration was performed with 10 and 2 kDa membranes, the obtained permeate was labeled as P1 and P2, respectively. Permeate of 2 kDa (P2) was further passed through a 150-Da membrane, and

retentate (R3) and permeate (P3) were collected. The volumes passing through different membranes for a particular time were recorded to calculate the flux. The collected permeate and retentate were analyzed using HPLC for the XOS and inhibitor content.

2.3.2. Activated Charcoal-Mediated purification (ACMP) of XOS. Hydrolysate obtained through the OAAH-3 treatment was subjected to centrifugation at 6000 rpm for 10 min. AC (3, 6, 9, 12, and 15% (w/v)) was added to the supernatant and stirred at 200 rpm for 1 h at room temperature. After centrifugation, the supernatant was discarded and the pellet was washed with MQ water twice to remove unbound impurities. Gradient elution with ethanol at 15, 30, 45, and 60% (v/v) concentrations was carried out to optimize the elution of xylooligosaccharide. The eluted fractions were concentrated using a rotary vacuum evaporator, and HPLC was performed to quantify XOS, free monosaccharides (xylose, arabinose, and glucose), and inhibitors (acetic acid, furfural, and hydroxymethylfurfural (HMF)). The functional groups of the AC used in this study were analyzed by Fourier Transform Infrared (FTIR, Tensor II, Bruker) spectroscopy for the spectrum range of 400–4000 cm^{-1} at a resolution of 4 cm^{-1} .

2.3.3. Graphene Oxide-Mediated Purification (GOMP) of XOS. The GO used in this study was synthesized and characterized in our previous work.^{27,30} The hydrolysate was treated with different concentrations of GO (1–5 mg/mL). The treated hydrolysate was incubated at 200 rpm for 1 h at room temperature. After incubation, the hydrolysate was centrifuged at 7000 rpm for 10 min, and both pellet and supernatant were collected. The pellet was further treated with different concentrations of ethanol (15, 30, 45, and 60%) in order to elute the adsorbed molecules. All the ethanol eluates were collected, vacuum-dried, and stored at –20 °C until further characterization. The supernatant containing the unabsorbed molecules and the ethanol-eluted pellet was further characterized using HPLC.¹⁴ FTIR (FTIR, Tensor II, Bruker) analysis with a spectrum range of 400–4000 cm^{-1} and a resolution of 4 cm^{-1} , was carried out, and purified XOS was described and compared with XOS in the OAAH hydrolysate. Scanning electron microscopy (SEM) analysis was also performed to get more structural insights into the materials used for XOS purification. The samples were prepared on a coverslip without adding any fixative agent and dehydrated at 37 °C for several hours and SEM images were captured under different magnifications to get a comprehensive picture of the test sample.³¹

2.4. Evaluation of Prebiotic Potential. The modified MRS base was prepared by mixing 1 g of protease peptone, 1 g of beef extract, 0.5 g of yeast extract, 0.1 g of polysorbate 80, 0.2 g of triammonium citrate, 0.5 g of sodium acetate, 0.01 g of magnesium sulfate, 0.005 g of manganese sulfate, and 0.2 g of dipotassium phosphate except for any carbon source. In order to study the growth curve of bacteria with XOS, GOMP-purified XOS was provided at a concentration of 2 mg/mL and was compared to dextrose at the same concentration. This MRS base was also supplemented with GOMP-XOS and ACMP-purified XOS at different concentrations (0.125, 0.25, 0.5, 1, and 2 mg/mL) to evaluate their growth stimulation after the treatment process. In both cases, growth stimulation was compared to dextrose (2 mg/mL) as a control.

The growth stimulatory effect of obtained XOS was studied by the standard plate count method as per the protocol described by Shubha et al., 2021, with minor modifications.³²

In brief, the LAB cultures (*L. acidophilus*, *L. casei*, *L. plantarum*, and *L. rhamnosus*) were grown individually in the medium and incubated at 37 °C for 24 h anaerobically. After the incubation, the number of colonies was counted with the help of a colony counter, and the growth was calculated as log CFU/mL. The % utilization of XOS by the tested bacteria was quantified by HPLC based on residual XOS in the medium by using the following equation.

$$\text{XOS utilisation (\%)} = \frac{\text{XOS}^{(\text{initial})} - \text{XOS}^{(\text{residual})}}{\text{XOS}^{(\text{initial})}} \times 100$$

2.5. XOS DP Utilization. The amount of XOS utilized in 24 h of incubation by different LAB cultures was estimated through HPLC using the method reported in our previous study.¹⁴ Briefly, the samples for HPLC were prepared by taking 1 mL of fermentation broth in microcentrifuge tubes and centrifuged at 6000 rpm for 10 min. Further, the supernatant was collected and filtered through a 0.22 μm sterile syringe filter (Acrodisc, PALL). Detection of oligomers was performed by using a Rezex™ RSO oligosaccharide Ag+ 4% column (200 mm × 10.0 mm, Phenomenex) at an oven temperature of 60 °C with a refractive index detector (2414) at 40 °C. HPLC grade water (Merck Life Science, India) was used as the mobile phase, with a flow rate of 0.25 mL/min. The results of the preferential utilization of XOS DP oligomers are presented as % utilization based on residual XOS (mg/mL) present in the medium after 24 h incubation.

2.6. SCFA Profiling of Fermented Product. The quantitative analysis of short-chain fatty acids (acetic acid, propionic acid, and butyric acid) and other organic acids (formic acid, lactic acid, and isovaleric acid) was carried out by using HPLC (10A-vp) with a system connected with a C18G (250 mm × 4.6 mm, 5 μm) column. Detection was carried out by using a photodiode array detector (SPD-M10Avp) at a 210 nm UV detection wavelength. For quantification of total SCFA in response to different substrates, calibration curves of acetic acid, lactic acid, propionic acid, butyric acid, formic acid, and isovaleric acid were prepared for concentrations of 10–100 mM, and the result was interpreted in terms of total SCFA as follows

$$\text{total SCFA} = A + B + P + L$$

where A is acetate, B is butyrate, P is propionate, and L is lactate.

Other organic acid quantification was also carried out by using standard curves of concentration ranging from 10 to 100 mM.

2.7. Statistical Analysis. The data presented here are the mean of three repetitions, including the standard deviation. The statistical analysis was carried out using the cloud-based Datatab platform, and the results were presented using DataGraph 5.0.

3. RESULTS AND DISCUSSION

3.1. XOS Purification by GOMP and Comparison with Membrane Filtration and ACMP. Autohydrolysis and acid/alkali treatment have been explored for XOS production from the lignocellulosic material (LCM). Nonselective breakdown of such LCM, results in the generation of impurities arising by partial hydrolysis of plant cell wall polysaccharides. As a consequence, downstream processing removal of such degradation products, and residual chemicals used in the

pretreatment along with good XOS recovery becomes a major challenge. For refinement and purification of XOS, solvent extraction, chromatography, and membrane filtration-based approaches have been evaluated, which tend to increase the cost of production on a commercial scale. As a result, there is a need for alternate methods that are environmentally friendly and can increase the purity as well as recovery of XOS.

In our previous work, we investigated the application of ozone-assisted autohydrolysis for increasing the yield of XOS production from lignocellulosic biomass, namely, wheat bran, and obtained a yield of 8.9% (w/w biomass).¹⁴ In this study, we explored a novel GOMP technique and compared it with two conventional methods used for the purification of XOS, namely, membrane filtration and AC.

3.1.1. Membrane Filtration-Mediated Purification (MFMP). The OAAH fraction (described in M&M) was subjected to sequential membrane purification for the removal of impurities (mainly plant cell wall polysaccharide degradation-derived compounds) and inhibitors. The details for MFMP along with the size of the membrane filters used, are presented in Scheme 1. The membrane permeate flux is represented in Table S1. Results indicated that the permeate (P1) obtained through the 10 kDa membrane resulted in a 32.39% recovery of total XOS from the hydrolysate. Permeate P1 was used as a feed for the 2 kDa membrane and recovery of XOS in permeate (P2) obtained was found to be 28.27% (XOS loss increased by 4.12%). After passing 70% of the volume of permeate (P2) through the final cutoff of 150 Da, the total recovery in retentate of XOS was 44.07% ± 0.92 in comparison with the initial XOS concentration (mg/mL) in the hydrolysate (Tables 1 and S2). We observed that the obtained

Table 1. Composition Analysis of the GOMP-Derived XOS (mg/mg) on a Dry Weight Basis (w/w) (n = 3)

composition	GOMP-XOS (%)
DP6	11.7 ± 0.3
DP5	4.2 ± 0.1
DP4	18.7 ± 0.6
DP3	57.8 ± 1.2
Dp2	3.7 ± 0.1
total XOS (DP2–5)	96.1 ± 1.7
xylose	1.2 ± 0.03
glucose	1.5 ± 0.04
furfural	0.01 ± 0.02
HMF	0.003 ± 0.01
AA	0.1 ± 0.03
unidentified	0.9 ± 0.02

efficiency of XOS recovery through membrane purification was not satisfactory. Clogging of the membrane because of unhydrolyzed xylan and higher length polysaccharide could be one possible reason for the initial loss of XOS in permeate (P1) obtained, especially through 10 kDa filtration.

3.1.2. Activated Charcoal-Mediated Purification. The adsorption behavior of different molecules towards AC has been utilized in oligosaccharide purification with ethanol elution. In our study, we observed that elution with different concentrations of ethanol resulted in the differential recovery of oligosaccharides in the eluate. A maximum recovery of 27.3 ± 0.49% XOS (DP2–6) was observed with the fraction eluted once using 15% ethanol. Three times elution by 15% ethanol, led to a total recovery of 72.7 ± 0.8% XOS (DP 2–6) (Figure

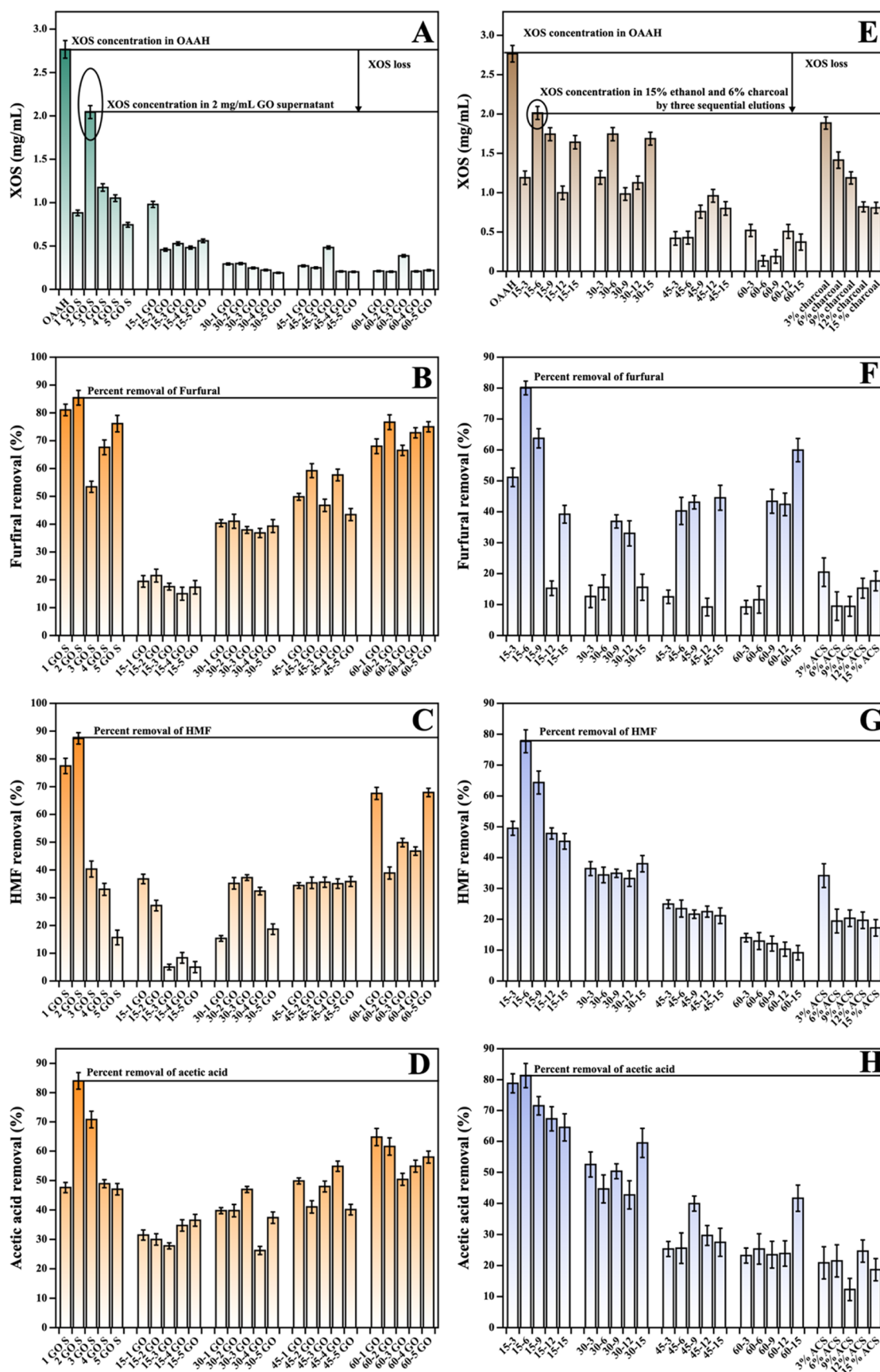


Figure 1. XOS purification by ACMP and GOMP. (A) Total XOS recovered after GO treatment. The removal of inhibitors from OAAH fraction by GO treatment (B) furfural, (C) HMF, and (D) acetic acid. (E) Total XOS recovered after AC treatment. The removal of inhibitors from the OAAH fraction by AC treatment (F) furfural, (G) HMF, and (H) acetic acid. (Values are mean \pm SD, $n = 3$).

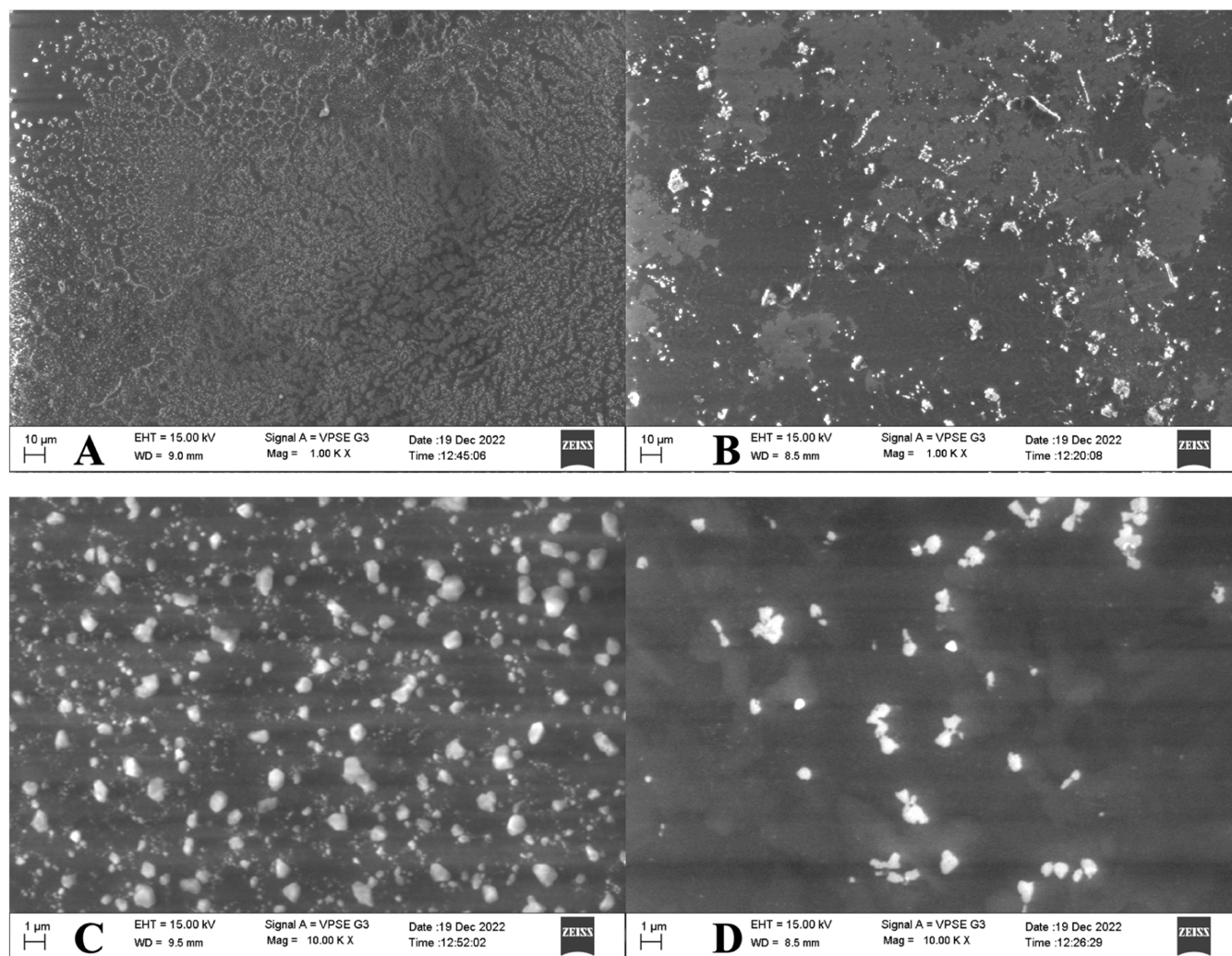


Figure 2. Characterization of GO and AC by SEM. Scanning electron microscopy images of AC (A, C) and GO (B, D) at different magnifications.

1E). There was also a significant decrease in inhibitors, namely furfural ($80.0 \pm 2.2\%$), HMF ($77.7 \pm 3.7\%$), and acetic acid ($81.3 \pm 3.9\%$), when OAAH was subjected to ACMP purification followed by three times ethanol elution for recovery. Results presented (Figure 1F,G,H) clearly indicate the efficient removal of inhibitors from hydrolysate after treatment with AC followed by gradient ethanol elution. In addition, a small amount of monosaccharide removal was also observed. This could be possible because, in comparison with monosaccharides and inhibitors, long-chain saccharides have a high potential to adsorb with charcoal and monosaccharides have weak adsorption capacity toward AC. For saccharides, it is reported that a higher degree of polymerization has a higher capacity to adsorb with AC.³³ FTIR analysis of AC showed that it consists of O–H ($3500\text{--}3200\text{ cm}^{-1}$), C=O ($1820\text{--}1600\text{ cm}^{-1}$), C=C ($1500\text{--}1400\text{ cm}^{-1}$), C–H ($3000\text{--}2850\text{ cm}^{-1}$), N=O ($1550\text{--}1350\text{ cm}^{-1}$), and C–N ($1350\text{--}1000\text{ cm}^{-1}$) functional groups (Figure 2A). Functional groups present on the surface play a crucial role in the selective adsorption as well as adsorption kinetic properties of the adsorbent material and could be modified according to its application (Maulina and Mentari, 2019). The scanning electron microscopy images of AC also confirm the more porous nature of AC than GO (Figure 2C,E).

3.1.3. Graphene Oxide-Mediated Purification. GO possesses a functional surface with a high number of oxygen-containing (polar) groups including hydroxyl and epoxy groups distributed in the plane whereas carboxyl groups are at the edges. The presence of such functional groups offers hydrophilicity to GO and in the presence of water, the carboxyl group gets hydrolyzed to acid, providing a negative charge to GO.³⁴ GO was used to remove the impurities and inhibitors from the OAAH hydrolysate. Results indicated that at a concentration of 2 mg/mL, GO did not adsorb XOS, and $73.87 \pm 4.25\%$ of XOS was retained in the supernatant (Figure 1A). The total XOS recovery after GOMP was found to be 1.676 and 1.015-fold higher than those after MFMP and ACMP, respectively. The supernatant also did not show the presence of inhibitors. This clearly suggested that impurities and inhibitors present in the hydrolysate adsorbed onto the GO surface. In order to confirm this observation, we subjected the mixture to gradient ethanol elution (15, 30, 45, 60%), which is known to remove adsorbed molecules from the GO surface. The results were as expected, and we found that in the presence of ethanol, the inhibitors desorbed from the functional surface. The rate of desorption of inhibitors was directly proportional to the concentration of ethanol used. As the concentration of ethanol increased from 15 to 60%, the rate of desorption of the inhibitors also increased consistently.

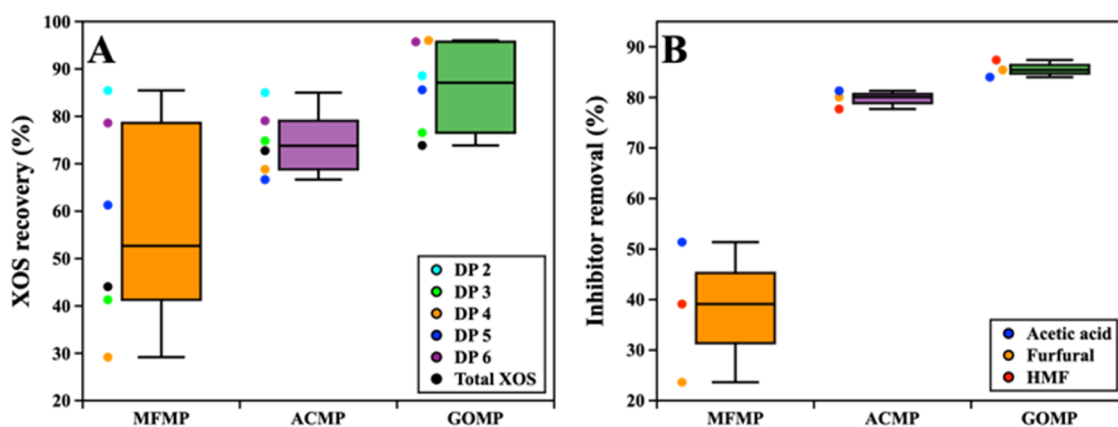


Figure 3. Statistical analysis of XOS recovery and inhibitor removal by different purification approaches. The box plot represents (A) XOS recovery and (B) inhibitor removal after purification.

The optimum concentration of GO was found to be 2 mg/mL to adsorb and remove acetic acid, furfural, and HMF at concentrations of 84.00 ± 2.837 , 85.42 ± 2.64 , and $87.38 \pm 2.04\%$, respectively (Figure 1B–D). The removal of acetic acid increased by 1.63 and 1.03-fold in GOMP compared to MFMP and ACMP, respectively. Furfural removal by GOMP was 3.61 and 1.06-fold higher than those of MFMP and ACMP. Further, the removal of HMF was found to increase in GOMP by 2.23 and 1.12-fold higher than MFMP and ACMP, respectively (Tables 1 and S3). The removal or extraction of furfural by using GO and catalysis of HMF has also been reported previously.^{28,35,36} Further, GO is reported to increase the hydrophilicity of the materials when used in membrane filtration by increasing the water transport and also acting as the antifouling agent. The functional groups present on the GO surface make it more dispersed in the polymeric solutions.³⁷

The characterization of GO performed by FTIR suggests that the oxide form of graphene possesses more oxygen-containing functional groups in the form of O–H ($3500\text{--}3200\text{ cm}^{-1}$), C=O ($1820\text{--}1600\text{ cm}^{-1}$), and C–O (Figure 2A). The nitrogen group-containing inhibitors, exhibits a strong affinity toward high oxygen-containing functional groups present on the GO surface. These functional groups were found to be in lesser amounts in the AC along with the abundance of C=N (Figure 2B), which favors the binding of XOS to the AC and not the inhibitors. On the other hand, the GO matrix removes the inhibitors from the hydrolysate by adsorption chemistry efficiently. In addition, SEM analysis also revealed that GO present in two-dimensional wrinkle sheets and nonporous structures provides more surface area than AC (Figure 2D,F). The AC was found to be highly porous and randomly distributed leading to a comparatively lesser surface area for adsorption (Figure 2C,E).

The adsorption property of GO has been previously explored extensively for the removal of organic contaminants, such as pesticides, dyes, and polycyclic aromatic hydrocarbons. It is also well-reported for use in the food industry as packaging materials. GO at a concentration of 4 mg/mL has been used for the removal of earthy odor contaminants (2-methyl isoborneol (MIB) and geosmin) generally found in surface water. The authors reported that the presence of an open-layered structure of GO favors the rate of adsorption of GO more than AC and this occurs mainly through hydrophobic interactions. This result clearly indicates that the hydro-

phobicity of the molecule plays an important role in adsorption and it is directly proportional to GO adsorption kinetics.³⁸ As 40% surface area of GO is occupied only by oxygen groups and bears an average negative charge of the order of 10 mC m^{-2} , it may be more adsorbent than AC and provides unique properties.³⁹ Also, the presence of oxygen-containing groups (pyrone, quinone, and carboxylic) in GO provides an acidic nature to the surface, while aromatic carbon rings such as nitrogen-rich moieties provide basicity to the carbon material. Different interactions mainly involved in the mechanism of adsorption are bond formation, $\pi\text{--}\pi/\pi\text{--}\pi$ interactions, and hydrophobic and electrostatic interactions.⁴⁰

A process that is economical, uses less harmful chemicals for synthesis, uses safer extractants, has a safer chemical design, uses renewable raw materials, is biodegradable, is an efficient biocatalyst, provides chemical safety, and is real-time are technological procedures known to be green methods.⁴¹ Our results also indicate the promising potential of GO for the significant removal of the inhibitors from the hydrolysate, with maximum recovery in total XOS along with lower oligomers. As GO is a metal-free and toxic chemical-free matrix, its use in the purification strategy makes it an eco-friendly approach with good efficacy. According to our findings, GOMP is better than ACMP because of the selective adsorption of inhibitor molecules on GO, not requiring the multiple steps of ethanol elution, unlike AC. The minimum XOS recovery and presence of inhibitors after purification of hydrolysate through MFMP makes it unsuitable for XOS purification without a pretreatment. Moreover, it uses energy for pressure generation and also has limitations of filter fouling apart from being cost-intensive. Further downstream processing is reduced in GOMP, which is essential in ACMP, particularly for the removal of ethanol. GOMP not only increases XOS recovery but is also efficient in the removal of the inhibitors compared to both conventional methods (MFMP and ACMP). The ultrasensitivity of GO to separate the inhibitor molecules from the hydrolysate and enhance XOS purification makes GOMP not only a promising technique but also a green alternative to be used for a wide range of hydrolysates containing small molecules like furfural and HMF.⁴²

3.1.4. Statistical Analysis. One-factor variance analysis for XOS recovery using ANOVA indicated a significant difference between the variables ($F = 6.27$, $p = 0.01$). A Bonferroni post hoc test was used to compare the groups in pairs to find out those which were significantly different. The Bonferroni post

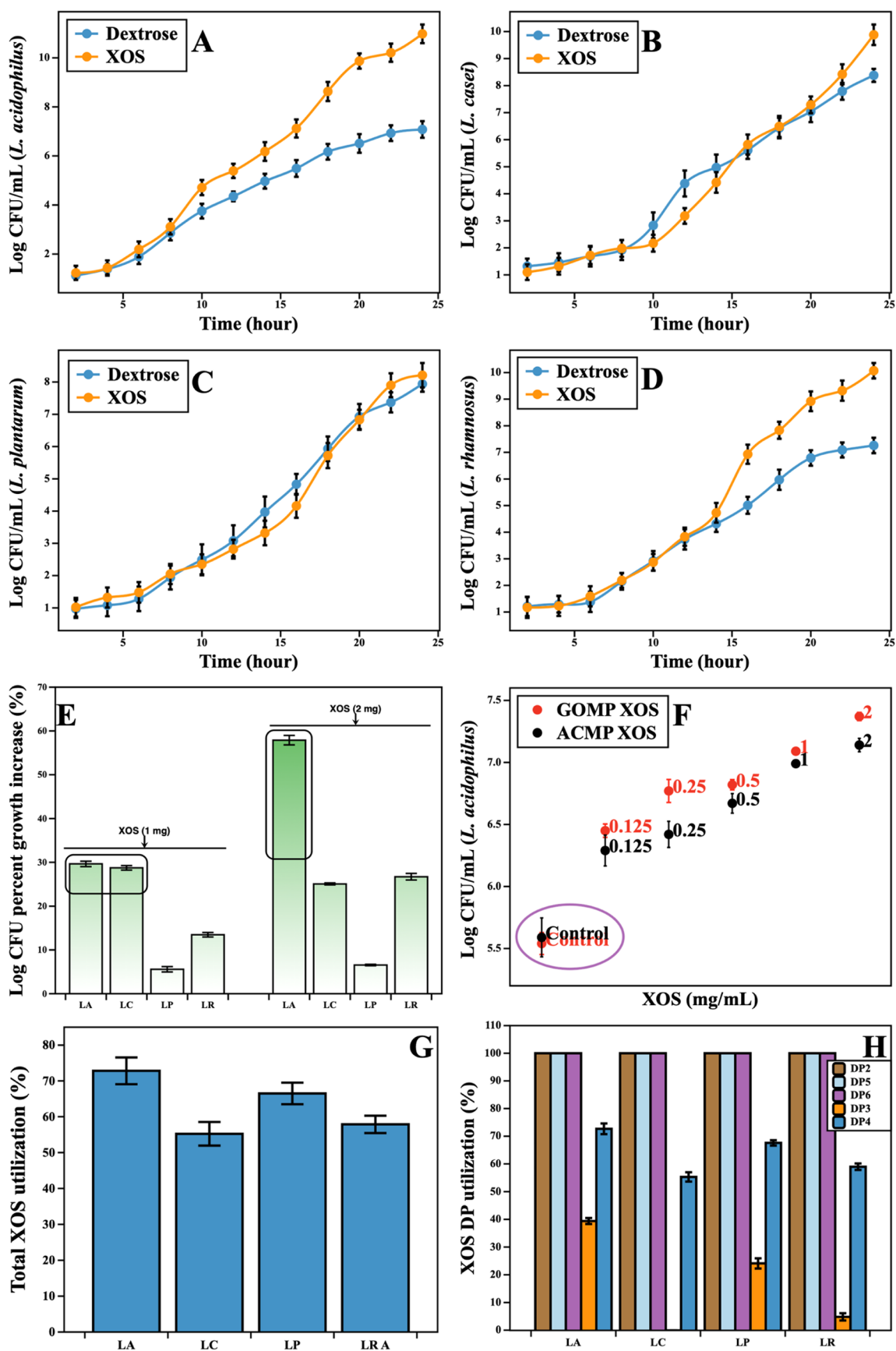


Figure 4. LAB growth studies and XOS preferential utilization. The growth curves of LAB with supplementation of XOS and dextrose for 24 h (A) *L. acidophilus*, (B) *L. casei*, (C) *L. plantarum*, and (D) *L. rhamnosus*. (E) Percentage change in growth of LAB (log CFU/mL) after 24 h in comparison with control. (F) Concentration-dependent effect of XOS obtained by GOMP and ACMP on LAB (G) Total XOS utilization of the bacteria and (H) XOS DP utilization by tested bacteria (values are mean \pm SD, $n = 3$).

Table 2. Organic Acid Production (mM) by Different LAB Cultures in a Medium Supplemented with XOS (2 mg/mL) as a Carbon Source

LAB	supplement	FA	LA	AA	PA	BA	IVA	total
LA	control	30.18 ± 1.84	453.23 ± 2.7	ND	37.59 ± 1.84	27.45 ± 1.73	ND	518.28 ± 5.62
	XOS	14.61 ± 0.84	75.53 ± 1.04	695.32 ± 3.75	76.23 ± 1.84	3.59 ± 0.74	33.59 ± 1.74	884.28 ± 5.83
LC	control	ND	ND	193.68 ± 2.64	ND	ND	ND	193.68 ± 2.74
	XOS	ND	ND	145.15 ± 1.94	3.11 ± 0.84	ND	ND	148.27 ± 3.05
LP	control	24.11 ± 1.93	4.85 ± 0.48	415.77 ± 3.75	119.92 ± 2.84	0.91 ± 0.03	ND	565.57 ± 6.84
	XOS	6.47 ± 0.847	ND	521.83 ± 4.73	41.56 ± 1.84	16.03 ± 0.38	21.39 ± 0.27	607.27 ± 5.83
LR	control	ND	ND	342.46 ± 3.84	3.08 ± 0.32	82.22 ± 1.73	ND	427.77 ± 7.73
	XOS	ND	ND	666.56 ± 4.82	3.10 ± 0.93	7.39 ± 0.52	ND	677.07 ± 6.93

hoc test showed that the pairwise group comparison of MFMP and GOMP for XOS recovery had a *p*-value of less than 0.05, and thus, based on the available data, the two groups were found to be significantly different (Figure 3A). A one-factor variance analysis for inhibitor removal also showed a significant difference between the variables ($F = 30.29$, $p = 0.001$). The Bonferroni post hoc test revealed that the pairwise group comparisons of MFMP–ACMP and MFMP–GOMP have a *p*-value less than 0.05 and thus, based on available data, these groups were found to be significantly different (Figure 3B).

3.1.5. Characterization of GOMP-Purified XOS. The XOS obtained after GOMP purification was further characterized by FTIR spectroscopy and LC-MS-MS technique for functional and structural change in the XOS (Figure S2). FTIR spectroscopy reveals that the XOS obtained after OAAH treatment was found to be in oxidized form due to the strong ozone treatment. The major molecules identified by LC-MS in the hydrolysate along with XOS were found to be glucose, xylose, and acetyl groups. The GOMP purification of XOS shows the maximum removal of monomers and other impurities present in the sample.

3.2. In Vitro Fermentation of XOS by Probiotic Bacteria. In order to ascertain that the obtained GOMP-purified XOS retains all the functional properties of a prebiotic, it was evaluated for its growth stimulatory effect on probiotic bacteria, utilization of the oligomers, and also the generation of bioactive metabolites.

The growth curve of LAB was studied with the supplementation of XOS and dextrose individually, over an incubation period of 24 h. Results indicated that *L. plantarum* and *L. casei* did not show a significant change in growth behavior when XOS was supplemented instead of dextrose (Figure 4B,C). *L. rhamnosus* indicated an improved growth performance with the supplementation of XOS after 14 h, which suggests that it requires a longer lag phase to initiate utilizing XOS as a substrate (Figure 4D). The growth of *L. acidophilus* in the presence of XOS was significantly higher than that of all other tested LAB. *L. acidophilus* indicated exponential growth in the presence of XOS in 8 h, which was lower than all other cultures (Figure 4A). A smaller lag phase and maximum growth in comparison to dextrose as substrate indicate *L. acidophilus* to be a prominent XOS utilizer.

Furthermore, the increase in the percentage of log CFU/mL was calculated for 24 h of incubation. A concentration-dependent increase in the growth of *L. acidophilus* was observed with XOS concentration indicating a 57.9% increase at 2 mg/mL XOS in comparison to growth in the control medium. Similarly, in the case of *L. plantarum* and *L. rhamnosus*, the highest growth was observed in XOS-supplemented with 2 mg/mL which was 6.5% and 26.8%,

respectively, in comparison to the control. In the case of *L. casei*, the highest increase in growth of 28.8% was observed at 1 mg/mL concentration, which was found to decrease to 25%, when XOS concentration was further increased to 2 mg/mL (Figure 4E). The concentration-dependent growth study performed on the *L. acidophilus* by XOS obtained by ACMP and GOMP suggests that XOS obtained after GOMP purification enhances the growth of *L. acidophilus* at all tested concentrations (Figure 4F).

In a study conducted by Pinpanit et al., 2021, the prebiotic potential of corn-cob-derived XOS (30 mg/mL) was evaluated against *L. casei* (TISTR1463) and *L. plantarum* (TISTR1463) with respect to their growth, XOS utilization, and β -xylosidase production for 0 to 48 h. Results revealed that *L. plantarum* (TISTR1463) utilized XOS efficiently as the viability increased and was found to be 10.29 log CFU/mL with β -xylosidase activity (0.147 U/mL). Whereas, *L. casei* (TISTR1463) showed a viable cell count of 3.02 log CFU/mL with β -xylosidase activity (0.15 U/mL).⁴³ Therefore, the study indicates and supports our observation that a higher XOS concentration does not further enhance the growth in the case of *L. casei*.

3.2.1. XOS DP Utilization Study by LAB. The utilization of XOS with respect to different oligomers (degree of polymerization) was performed on LAB to get insight into the utilization pattern of XOS. Figure 4G clearly indicates that after 24 h of incubation, *L. acidophilus* consumed $72.81 \pm 0.018\%$ (0.73 mg/mL) of XOS (DP2 to DP6) including xylose. While *L. plantarum* efficiently utilized $66.49 \pm 0.021\%$ (0.33 mg/mL) of available XOS compared to other LAB bacteria (*L. casei*–55.14 ± 0.028%, *L. rhamnosus*–60.11 ± 0.028%) (Figure 4G,H). As xylose, DP2, DP5, and DP6 were not detected in the postfermented supernatant because of their very low concentration in total XOS, the result indicated their efficient utilization by LAB within 24 h. Results presented in Figure 4H show that DP3 and DP4 consumption is also very high by *L. acidophilus* and a similar trend of utilization is observed in the case of *L. plantarum*. Efficient utilization of DP4 is found to be more in all LAB while DP3 consumption was found to be less in the case of *L. casei* and *L. rhamnosus*, indicating a variation in DP preference for XOS utilization. In a nutshell, there was differential utilization of XOS oligomers by the LAB, which was both DP and culture-dependent. Along with xylanase, efficient utilization of XOS depends on the cooperative action of different enzymes such as acetyl xylan esterase, α -glucuronidase, β -xylosidase, and α -L-arabinofuranosidase, which indicates XOS utilization is mainly decided by the xylanolytic enzyme systems. Also, the basic reason for such variation in response of LAB toward XOS could be that specific β -xylosidase activity is expressed in a different manner

in *Lactobacillus* spp. cultures.⁴⁴ Hence, prebiotic activity exhibited by XOS is always a result of the variation in the arabinose to xylose ratio, degree of polymerization of oligomers, substitution associated with oligomer, and type of strain used.

3.2.2. SCFA Profiling. The results of the organic acids produced by the different bacterial cultures after XOS utilization are listed in Table 2. Interestingly, acetic acid was found to increase with XOS supplementation in the case of *L. acidophilus*, *L. plantarum*, and *L. rhamnosus* compared to the control, except in the case of *L. casei*. Whereas, lactic acid and formic acid productions were observed only in *L. acidophilus* and *L. plantarum*, and it was found to be higher in control compared to XOS as a carbon source. Butyric acid and isovaleric acid production was found to be enhanced with supplementation of XOS only in the case of *L. plantarum* and *L. acidophilus*. The isovaleric acid comes under the branched SCFA, which has been reported for its direct impact on adipocyte glucose and lipid metabolism.⁴⁵ Propionic acid was higher in all tested LAB in the presence of XOS except in the case of *L. plantarum*. In the case of *L. acidophilus*, the production of lactic acid was reduced 6-fold in the presence of the XOS while the production of propionic acid increased by 2.02-fold, and acetic acid increased dramatically as it is absent in the control. As pyruvate and lactate can be converted into acetate by pyruvate dehydrogenase, acetate kinase, phosphotransacetylase, and LDH-POX-ACK pathways, respectively, acetate has been found as an end product, and therefore, is possibly present at the later exponential growth phase and remains in the stationary phase.⁴⁶ It is well-reported that change in the SCFA profile directly affects the brain, immune system, and the gut-system. The SCFA mainly contributes to the homeostasis of the gut-brain integrity, inflammatory response, regulates the immune system, and lipid and glucose metabolism.⁴⁷

The ratio between acetic acid, propionic acid, and butyric acid (AA:PA:BA) was individually calculated for all pure LAB cultures, with XOS supplementation. SCFA ratios were calculated as, 89.7:9.8:0.46 (*L. acidophilus*), 97.89:2.1:0 (*L. casei*), 90:7.1:2.7 (*L. plantarum*), and 98.4:0.45:1 (*L. rhamnosus*), which was found to be different from the control. The butyrate production in XOS-supplemented *L. plantarum* and *L. rhamnosus* was found to be reduced by 7.64- and 11.12-fold, respectively, compared to dextrose supplementation. In the case of *L. casei*, we did not observe the production of the butyrate in both control and XOS supplementation. Whereas, we found that in *L. plantarum*, the production of butyrate increased with XOS supplementation by 17.61-fold as compared with dextrose. The production of butyrate in the presence of dextrose has already been reported for *L. plantarum* and *L. rhamnosus*.^{48,49} The results support the previous literature studies that *Lactobacillus* can not only produce lactic acid but also is involved in the fermentation or biotransformation of lactic acid into other organic acids. An appreciable amount of SCFA and other organic acid production in the presence of XOS supplementation imparts a beneficial effect on colon health by inhibiting the colonization of pathogens and playing a crucial role in other metabolites' activities.

4. CONCLUSIONS

In our study, membrane purification was found to be less efficient for XOS purification with a loss of 55.92% of total

XOS from the hydrolysate obtained after autohydrolysis. The GOMP approach outperformed membrane filtration, recovering $73.87 \pm 4.25\%$ of the XOS and significantly removing the autogenerated inhibitors. Also, the one-step GOMP method did not require the use of ethanol elution of XOS, unlike AC. The acquired XOS also showed promising prebiotic properties with respect to LAB growth and SCFA profiles. These findings provide evidence of our proposed hypothesis that GO preferentially interacts and adsorb autogenerated inhibitors during autohydrolysis treatment, enabling purification and concentration of XOS while also preserving its prebiotic potential by eliminating the inhibitors. The enhanced XOS recovery together with inhibitor removal by GOMP, opens up new avenues for XOS as well as oligosaccharide purification on a commercial scale.

■ ASSOCIATED CONTENT

Supporting Information

The Supporting Information is available free of charge at <https://pubs.acs.org/doi/10.1021/acsomega.3c05714>.

Representative HPLC chromatograms of XOS; the membrane permeates flux (L/m²/h) of the OAAH hydrolysate; XOS DP distribution, total XOS (mg/mL), and XOS percent recovery by MFMP; FTIR spectra of AC, GO, and XOS; comparison of the different processes used for XOS purification; LC-MS analysis of crude XOS and purified XOS; and growth stimulation study of XOS on LAB (PDF)

■ AUTHOR INFORMATION

Corresponding Author

Praveena Bhatt – Academy of Scientific and Innovative Research (AcSIR), Ghaziabad- 201002, India; Microbiology and Fermentation Technology Department, CSIR-Central Food Technological Research Institute, Mysore 570020, India; orcid.org/0000-0002-1522-1645;
Email: praveena@cftri.res.in

Authors

Rutuja Murlidhar Sonkar – Academy of Scientific and Innovative Research (AcSIR), Ghaziabad- 201002, India; Microbiology and Fermentation Technology Department, CSIR-Central Food Technological Research Institute, Mysore 570020, India

Pravin Savata Gade – Academy of Scientific and Innovative Research (AcSIR), Ghaziabad- 201002, India; Microbiology and Fermentation Technology Department, CSIR-Central Food Technological Research Institute, Mysore 570020, India

Sandeep N. Mudliar – Academy of Scientific and Innovative Research (AcSIR), Ghaziabad- 201002, India; Plant Cell Biotechnology Department, CSIR-Central Food Technological Research Institute, Mysore 570020, India

Complete contact information is available at: <https://pubs.acs.org/10.1021/acsomega.3c05714>

Author Contributions

All authors have given approval to the final version of the manuscript. R.M.S.: Conceptualization, design of experiments, experimentation, formal analysis, investigation, visualization, and writing-original draft; P.S.G.: Experimentation, visualization, and analysis; S.N.M.: Membrane purification studies, resources, reviewing, and editing P.B.: Conceptualization,

design of experiments, interpretation, resources, and reviewing and editing.

Notes

The authors declare no competing financial interest.

ACKNOWLEDGMENTS

The authors acknowledge the support from the Director CSIR-CFTRI, Mysuru. R.M.S. and P.S.G. would like to gratefully acknowledge the funding (JRF/SRF) support from the Department of Biotechnology (DBT) India.

REFERENCES

- (1) Adewuyi, A. Underutilized Lignocellulosic Waste as Sources of Feedstock for Biofuel Production in Developing Countries. *Front Energy Res.* **2022**, *10*, No. 741570.
- (2) Sadh, P. K.; Duhan, S.; Duhan, J. S. Agro-Industrial Wastes and Their Utilization Using Solid State Fermentation: A Review. *Bioresour. Bioprocess* **2018**, *5* (1), 1–15.
- (3) Narisetty, V.; Parhi, P.; Mohan, B.; Hakkim Hazeena, S.; Naresh Kumar, A.; Gullón, B.; Srivastava, A.; Nair, L. M.; Paul Alphy, M.; Sindhu, R.; Kumar, V.; Castro, E.; Kumar Awasthi, M.; Binod, P. Valorization of Renewable Resources to Functional Oligosaccharides: Recent Trends and Future Prospective. *Bioresour. Technol.* **2022**, *346*, No. 126590, DOI: 10.1016/j.biortech.2021.126590.
- (4) Chen, Y.; Xie, Y.; Ajuwon, K. M.; Zhong, R.; Li, T.; Chen, L.; Zhang, H.; Beckers, Y.; Everaert, N. Xylo-Oligosaccharides, Preparation and Application to Human and Animal Health: A Review. *Front. Nutr.* **2021**, *8*, No. 731930.
- (5) de Oliveira, S. M.; Moreno-Perez, S.; Terrasan, C. R. F.; Romero-Fernández, M.; Vieira, M. F.; Guisan, J. M.; Rocha-Martin, J. Covalent Immobilization-Stabilization of β -1,4-Endoxylanases from *Trichoderma Reesei*: Production of Xylooligosaccharides. *Process Biochem.* **2018**, *64*, 170–176.
- (6) Huang, L. Z.; Ma, M. G.; Ji, X. X.; Choi, S. E.; Si, C. Recent Developments and Applications of Hemicellulose From Wheat Straw: A Review. *Front. Bioeng. Biotechnol.* **2021**, *9*, No. 690773.
- (7) Bhatia, L.; Sarangi, P. K.; Singh, A. K.; Prakash, A.; Shadangi, K. P. Lignocellulosic Waste Biomass for Biohydrogen Production: Future Challenges and Bio-Economic Perspectives. *Biofuels, Bioprod. Biorefin.* **2021**, *838–858*.
- (8) FAO. *Crop Prospects and Food Situation #1, March 2022*; 2022. DOI: 10.4060/cb8893en.
- (9) Ruthes, A. C.; Martínez-Abad, A.; Tan, H. T.; Bulone, V.; Vilaplana, F. Sequential Fractionation of Feruloylated Hemicelluloses and Oligosaccharides from Wheat Bran Using Subcritical Water and Xylanolytic Enzymes. *Green Chem.* **2017**, *19* (8), 1919–1931.
- (10) Lian, Z.; Wang, Y.; Luo, J.; Lai, C.; Yong, Q.; Yu, S. An Integrated Process to Produce Prebiotic Xylooligosaccharides by Autohydrolysis, Nanofiltration and Endo-Xylanase from Alkali-Extracted Xylan. *Bioresour. Technol.* **2020**, *314* (159), No. 123685.
- (11) Silva, E. K.; Arruda, H. S.; Mekala, S.; Pastore, G. M.; Meireles, M. A. A.; Saldaña, M. D. A. Xylooligosaccharides and Their Chemical Stability under High-Pressure Processing Combined with Heat Treatment. *Food Hydrocolloids* **2022**, *124*, No. 107167, DOI: 10.1016/j.foodhyd.2021.107167.
- (12) Scapini, T.; dos Santos, M. S. N.; Bonatto, C.; Wancura, J. H. C.; Mulinari, J.; Camargo, A. F.; Klanovicz, N.; Zabot, G. L.; Tres, Mv.; Fongaro, G.; Treichel, H. Hydrothermal Pretreatment of Lignocellulosic Biomass for Hemicellulose Recovery. *Bioresour. Technol.* **2021**, *342*, No. 126033, DOI: 10.1016/j.biortech.2021.126033.
- (13) Poletto, P.; Pereira, G. N.; Monteiro, C. R. M.; Pereira, M. A. F.; Bordignon, S. E.; de Oliveira, D. Xylooligosaccharides: Transforming the Lignocellulosic Biomasses into Valuable 5-Carbon Sugar Prebiotics. *Process Biochem.* **2020**, *91*, 352–363, DOI: 10.1016/j.procbio.2020.01.005.
- (14) Sonkar, R. M.; Gade, P. S.; Vijay, B.; M S, N.; Bhatt, P. Ozone Assisted Autohydrolysis of Wheat Bran Enhances Xylooligosaccharide Production with Low Generation of Inhibitor Compounds: A Comparative Study. *Bioresour. Technol.* **2021**, *338*, No. 125559.
- (15) Guo, W.; Bruining, H. C.; Heeres, H. J.; Yue, J. Insights into the Reaction Network and Kinetics of Xylose Conversion over Combined Lewis/Brønsted Acid Catalysts in a Flow Microreactor. *Green Chem.* **2023**, *25*, 5878.
- (16) Xu, F.; Chen, J.; Yang, G.; Ji, X.; Wang, Q.; Liu, S.; Ni, Y. Combined Treatments Consisting of Calcium Hydroxide and Activate Carbon for Purification of Xylo-Oligosaccharides of Pre-Hydrolysis Liquor. *Polymers* **2019**, *11* (10), No. 1558.
- (17) Montané, D.; Nabarlaz, D.; Martorell, A.; Torné-Fernández, V.; Fierro, V. Removal of Lignin and Associated Impurities from Xylo-Oligosaccharides by Activated Carbon Adsorption. *Ind. Eng. Chem. Res.* **2006**, *45* (7), 2294–2302.
- (18) Chemat, F.; Abert Vian, M.; Fabiano-Tixier, A. S.; Nutrizio, M.; Režek Jambak, A.; Muneke, P. E. S.; Lorenzo, J. M.; Barba, F. J.; Binello, A.; Cravotto, G. A Review of Sustainable and Intensified Techniques for Extraction of Food and Natural Products. *Green Chem.* **2020**, *2325–2353*, DOI: 10.1039/c9gc03878g.
- (19) Wang, Y. H.; Zhang, J.; Qu, Y. S.; Li, H. Q. Removal of Chromophore in Enzymatic Hydrolysis by Acid Precipitation to Improve the Quality of Xylo-Oligosaccharides from Corn Stalk. *Bioresour. Technol.* **2018**, *249*, 751–757.
- (20) Shi, L. Bioactivities, Isolation and Purification Methods of Polysaccharides from Natural Products: A Review. *Int. J. Biol. Macromol.* **2016**, *92*, 37–48.
- (21) Li, X.; Tan, S.; Luo, J.; Pinelo, M. Nanofiltration for Separation and Purification of Saccharides from Biomass. *Front. Chem. Sci. Eng.* **2021**, *837–853*, DOI: 10.1007/s11705-020-2020-z.
- (22) Gibson, G. R.; Hutkins, R.; Sanders, M. E.; Prescott, S. L.; Reimer, R. A.; Salminen, S. J.; Scott, K.; Stanton, C.; Swanson, K. S.; Cani, P. D.; Verbeke, K.; Reid, G. Expert Consensus Document: The International Scientific Association for Probiotics and Prebiotics (ISAPP) Consensus Statement on the Definition and Scope of Prebiotics. *Nat. Rev. Gastroenterol. Hepatol.* **2017**, *14* (8), 491–502.
- (23) Palaniappan, A.; Antony, U.; Emmambux, M. N. Current Status of Xylooligosaccharides: Production, Characterization, Health Benefits and Food Application. *Trends Food Sci. Technol.* **2021**, *111*, 506–519.
- (24) Tang, S.; Chen, Y.; Deng, F.; Yan, X.; Zhong, R.; Meng, Q.; Liu, L.; Zhao, Y.; Zhang, S.; Chen, L.; Zhang, H. Xylooligosaccharide-Mediated Gut Microbiota Enhances Gut Barrier and Modulates Gut Immunity Associated with Alterations of Biological Processes in a Pig Model. *Carbohydr. Polym.* **2022**, *294*, No. 119776.
- (25) Almiro Mazive, P.; Hu, B.; Zhu, H.; He, W.; Menino Mazive, A. Graphene Oxide; Adsorption; Organic, Inorganic; Biological; Radiological Contaminants. *J. Nanotechnol. Res.* **2020**, *02* (04), 60–91, DOI: 10.26502/jnr.2688-85210017.
- (26) Marcano, D. C.; Kosynkin, Dv.; Berlin, J. M.; Sinitiskii, A.; Sun, Z.; Slesarev, A.; Alemany, L. B.; Lu, W.; Tour, J. M. Improved Synthesis of Graphene Oxide. *ACS Nano* **2010**, *4* (8), 4806–4814.
- (27) Gade, P. S.; Sonkar, R. M.; Bhatt, P. Graphene Oxide-Mediated Fluorescence Turn-on GO-FAM-FRET Aptasensor for Detection of Sterigmatocystin. *Anal. Methods* **2022**, *14*, 3890.
- (28) Antunes, M. M.; Russo, P. A.; Wiper, P.; Veiga, J. M.; Pillinger, M.; Mafra, L.; Evtuguin, Dv.; Pinna, N.; Valente, A. A. Sulfonated Graphene Oxide as Effective Catalyst for Conversion of 5-(Hydroxymethyl)-2-Furfural into Biofuels. *ChemSusChem* **2014**, *7* (3), 804–812.
- (29) Ghime, D.; Ghosh, P. Removal of Toxic Pollutants through Advanced Oxidation Processes. In *Removal of Toxic Pollutants Through Microbiological and Tertiary Treatment*; Shah, M. P., Ed.; Elsevier, 2020; Chapter 4, pp 139–151.
- (30) Reddy Gajjala, R. K.; Gade, P. S.; Bhatt, P.; Vishwakarma, N.; Singh, S. Enzyme Decorated Dendritic Bimetallic Nanocomposite Biosensor for Detection of HCHO. *Talanta* **2022**, *238* (P2), No. 123054.

- (31) Aisyah, N.; Rifai, H.; Maisonneuve, C. B. D.; La; Oalman, J.; Forni, F.; Eisele, S.; Phua, M.; Putra, R. Scanning Electron Microscope (SEM) Imaging and Analysis of Magnetic Minerals of Lake Diatas Peatland Section DD REP B 693. *J. Phys.: Conf. Ser.* **2020**, *1481*, No. 012025, DOI: 10.1088/1742-6596/1481/1/012025.
- (32) Shubha, J. R.; Tripathi, P.; Somashekar, B. S.; Kurrey, N.; Bhatt, P. Woodfordia Fruticosa Extract Supplementation Stimulates the Growth of Lacticaseibacillus Casei and Lacticaseibacillus Rhamnosus with Adapted Intracellular and Extracellular Metabolite Pool. *J. Appl. Microbiol.* **2021**, *131* (6), 2994–3007.
- (33) Kamollak Jirakulkanok(Kasetsart University, B. (Thailand). F. of A-Industry. D. of F. S. and T.; Ladda Sangduean Wattanasiritham(Kasetsart University, B. (Thailand). I. of F. R. and P. D.; Pinthip Rumpagaporn(Kasetsart University, B. (Thailand). F. of A-Industry. D. of F. S. and T. E. ac. th. Preparation and Purification of Oligosaccharides from Commercially Defatted Rice Bran. 2018.
- (34) Liu, Y. In *Application of Graphene Oxide in Water Treatment*, IOP Conference Series: Earth and Environmental Science; Institute of Physics Publishing, 2017.
- (35) Piñeiro-García, A.; González-Alatorre, G.; Vega-Díaz, S. M.; Pérez-Pérez, M. C. L.; Tristan, F.; Patiño-Herrera, R. Reduced Graphene Oxide Coating with High Performance for the Solid Phase Micro-Extraction of Furfural in Espresso Coffee. *Journal of Food Meas. Charact.* **2020**, *14* (1), 314–321.
- (36) Zhu, W.; Tao, F.; Chen, S.; Li, M.; Yang, Y.; Lv, G. Efficient Oxidative Transformation of Furfural into Succinic Acid over Acidic Metal-Free Graphene Oxide. *ACS Sustainable Chem. Eng.* **2019**, *7* (1), 296–305.
- (37) Woo, Y. C.; Kim, S.-H.; Shon, H. K.; Tijing, L. D. *Introduction: Membrane Desalination Today, Past, and Future*, 2018.
- (38) Hafuka, A.; Nagasato, T.; Yamamura, H. Application of Graphene Oxide for Adsorption Removal of Geosmin and 2-Methylisoborneol in the Presence of Natural Organic Matter. *Int. J. Environ. Res. Public Health* **2019**, *16* (11), No. 1907.
- (39) Nebol'sin, V. A.; Galstyan, V.; Silina, Y. E. Graphene Oxide and Its Chemical Nature: Multi-Stage Interactions between the Oxygen and Graphene. *Surf. Interfaces* **2020**, No. 100763, DOI: 10.1016/j.surf.2020.100763.
- (40) Smith, A. T.; LaChance, A. M.; Zeng, S.; Liu, B.; Sun, L. Synthesis, Properties, and Applications of Graphene Oxide/Reduced Graphene Oxide and Their Nanocomposites. *Nano Mater. Sci.* **2019**, *1* (1), 31–47.
- (41) Boateng, I. D. Evaluating the Status Quo of Deep Eutectic Solvent in Food Chemistry. Potentials and Limitations. *Food Chem.* **2023**, No. 135079, DOI: 10.1016/j.foodchem.2022.135079.
- (42) Morelos-Gomez, A.; Terashima, S.; Yamanaka, A.; Cruz-Silva, R.; Ortiz-Medina, J.; Sánchez-Salas, R.; Fajardo-Díaz, J. L.; Muñoz-Sandoval, E.; López-Urías, F.; Takeuchi, K.; Tejima, S.; Terrones, M.; Endo, M. Graphene Oxide Membranes for Lactose-Free Milk. *Carbon* **2021**, *181*, 118–129.
- (43) Boonchuay, P.; Wongpoomchai, R.; Jaturasitha, S.; Mahatheeranont, S.; Watanabe, M.; Chaiyaso, T. Prebiotic Properties, Antioxidant Activity, and Acute Oral Toxicity of Xylooligosaccharides Derived Enzymatically from Corncob. *Food Biosci* **2021**, *40*, No. 100895.
- (44) Chapla, D.; Pandit, P.; Shah, A. Production of Xylooligosaccharides from Corncob Xylan by Fungal Xylanase and Their Utilization by Probiotics. *Bioresour. Technol.* **2012**, *115*, 215–221.
- (45) Heimann, E.; Nyman, M.; Pålbrink, A. K.; Lindkvist-Petersson, K.; Degerman, E. Branched Short-Chain Fatty Acids Modulate Glucose and Lipid Metabolism in Primary Adipocytes. *Adipocyte* **2016**, *5* (4), 359–368.
- (46) Slavica, A.; Trontel, A.; Jelovac, N.; Kosovec, Ž.; Šantek, B.; Novak, S. Production of Lactate and Acetate by Lactobacillus Coryniformis Subsp. Torquens DSM 20004T in Comparison with Lactobacillus Amylovorus DSM 20531T. *J. Biotechnol.* **2015**, *202*, 50–59.
- (47) Nogal, A.; Valdes, A. M.; Menni, C. The Role of Short-Chain Fatty Acids in the Interplay between Gut Microbiota and Diet in Cardio-Metabolic Health. *Gut Microb.* **2021**, 1–24, DOI: 10.1080/19490976.2021.1897212.
- (48) Thananimit, S.; Pahumunto, N.; Teanpaisan, R. Characterization of Short Chain Fatty Acids Produced by Selected Potential Probiotic Lactobacillus Strains. *Biomolecules* **2022**, *12* (12), No. 1829.
- (49) Pessione, A.; Lo Bianco, G.; Mangiapane, E.; Cirrincione, S.; Pessione, E. Characterization of Potentially Probiotic Lactic Acid Bacteria Isolated from Olives: Evaluation of Short Chain Fatty Acids Production and Analysis of the Extracellular Proteome. *Food Res. Int.* **2015**, *67*, 247–254.